

High Velocity Compaction and Sintering of Stellite 12 Powders

T. Berglund^{a,b}, M. Olsson^a

^a Dalarna University, SE-781 88 Borlänge, Sweden

^b SinterHeat, Box 2, SE-770 70 Långshyttan Sweden

Abstract It is known that gas atomized powders as well as highly alloyed metal powders are difficult to press into green bodies using conventional quasi static pressing techniques. However, the development of the high velocity compaction (HVC) technique has expanded the possibility to compact a larger spectrum of metal powders. Although the HVC technique has many similarities with conventional pressing techniques, e.g. the powder filling and ejection of the pressed components, the high energy impact makes it an interesting technique not only for the pressing of conventional metal powders to green bodies of high density but also for the pressing of "difficult to press metal powders" such as cobalt based alloys. Stellites are a series of cobalt based super alloys widely used for their high hardness, good tribological properties and good corrosion resistance and consequently there is an increased interest in the near net shape (NNS) manufacturing of Stellite components. In the present study gas and water atomized Stellite powders with a chemical composition corresponding to Stellite 12 has been compacted using the HVC technique. The compaction characteristics have been evaluated and the possibility of manufacturing high density green bodies investigated. Furthermore, two different sintering processes, i.e. sintering in argon and sintering in vacuum, have been evaluated. The as-sintered microstructures have been characterized and compared to the microstructure of an existing commercial pressed and sintered Stellite 12 alloy. The results show that high velocity compaction is well suited for the compaction of water atomized Stellite 12 powder to high green densities (95% of the relative theoretical density) although transfer of powder material on the die surfaces was observed at higher compaction energies, resulting in poor surface finish of the green bodies. In contrast, high velocity compaction of the agglomerated gas atomized Stellite 12 powder is associated with problems, mainly due to cracking and capping of the green bodies already at relatively low compaction energies. Sintering in vacuum results in a higher as-sintered density as compared with sintering in argon. Under both sintering conditions extra carbon needs to be added to the powder in order to compensate for carbon loss during the sintering process. However, in order to avoid a coarse microstructure, associated with a large grain size and the formation of eutectic carbides and carbide networks, having a negative impact on the resulting mechanical properties, the amount of liquid phase formed during sintering must be kept to a minimum. This is of importance in order to obtain a high hardness of the as-sintered material.

1 INTRODUCTION

Stellites are a series of cobalt base alloys developed by Elwood Haynes known for their high strength, high hot hardness and good wear and corrosion resistance. Furthermore many Stellites exhibit very low friction against most metals under dry sliding conditions. Stellites are generally alloyed with C, Cr, W and minor amounts of Si, Mn, Fe and Ni. Presently more and more of the W in Stellites are being replaced by Mo due to the lower cost of Mo and improvements in certain critical properties [1, 2]. The high strength, hot hardness and wear resistance are accomplished by the precipitation of a high amount of carbides in a matrix strengthened by solid solution of Cr, W and/or Mo. Several types of carbides can be found in Stellites, typically Cr-rich $M_{23}C_6$ and/or M_7C_3 carbides are found. In alloys with higher C and W or Mo content, M_6C carbides are also found [1,2,3,4]. The type of carbides present and their relative amounts depend on the alloying content of C, Cr, Mo and W. The good corrosion resistance mainly originates from the alloying with high amounts of Cr, typically between 25 and 30 wt.%. Although some of the Cr is present in the form of stable Cr-rich carbides, most remain in solid solution in the Co-rich matrix. The frequently observed low friction characteristics of Stellites are attributed to the formation of an easily sheared layer on top of a deformation hardened layer during sliding contact. The most studied of the Stellite alloys are Stellites 6, 12 and 706. Stellite 6 mainly consists of Cr-rich M_7C_3 and/or $M_{23}C_6$ carbides in a solid solution dominated by Co. Stellite 12 has a higher W-content and a slightly higher C-content than Stellite 6. Stellite 706 is a Mo-modification of Stellite 6 where much of the W has been replaced by Mo. High Velocity Compaction (HVC) is a powder pressing technique that through the application of a high energy impact presses the powder to very high densities, often significantly higher than that obtained using ordinary cold pressing techniques. Often techniques like warm pressing and double pressing must be utilized in order to reach the density levels that can be reached with HVC [5]. Highly alloyed metal powders that are known to be difficult to press are in most cases readily pressed to high green densities using HVC. While water atomized powders generally can be pressed without any problems the pressing of gas atomized powders are associated

with some difficulties. Firstly, the spherical shape of gas atomized particles reduces the interlocking between neighbor particles in the green body reducing the green strength. Secondly, the fact that most gas atomized powders are fully alloyed results in a high particle hardness which inhibits plastic deformation at the particle contacts and thereby the compaction. Also, since many gas atomized powders are agglomerated containing fairly high amounts of an organic binder may further reduce the strength of pressed green bodies. The aim of the present study is to investigate the possibility to utilize the high green density achievable by HVC to refine the microstructure of pressed and sintered Stellite 12. The goal is to be able to manufacture close to near net shape saw teeth from Stellite 12 powder using high velocity compaction to very high green densities and subsequent post sintering using a proper sintering cycle.

2 EXPERIMENTAL

2.1 Materials

Two different Stellite powders, an agglomerated gas atomized (g.a.) powder and a water atomized (w.a.) powder were included in the study, see Table I. Both powders have a composition corresponding to Stellite 12. The gas atomized powder was agglomerated using a starch based binder while the water atomized powder had 1 wt.% of wax admixed for lubrication during compaction. Besides, a bulk commercial Stellite 12 grade was included as a reference material for the characterization of as-sintered microstructures.

Table I. Stellite powders included in the present study.

Powder	Chemical composition [weight %]
Stellite 12 g.a.	1 Mn, 1.5 Si, 29.5 Cr, max 2.5 Fe, max 3 Ni, 8.5 W, bal Co, 1.4-1.85 C
Stellite 12 w.a.	1.1 Si, 29.2 Cr, 1.2 Fe, 1.5 Ni, 8.2 W, bal Co. (1.4 C)

2.2 High velocity compaction

In the present study, cylindrical samples with a diameter of 25 mm and a height of approximately 4 mm (corresponding to a powder weight of 25 g) were high velocity compacted with different compaction energies using a Hydropulsor HYP 35-4 HVC machine at SinterHeat AB, Sweden, with maximum compaction energy of 4 kJ. In the present study the compaction energy was gradually increased by increasing the hitting height (i.e. the acceleration distance) of the piston from 5 mm and up to 55 mm. A good approximation of the applied compaction energy E (for the used Hydropulsor HYP 35-4 machine) is $E = 46 \cdot S$ Joule, where S is the piston hitting height in mm, i.e. the compaction energies varied from 0.23 kJ and up. Besides the HVC tests, two series of samples for sintering was prepared for the water atomized powder, one with lower green density (hitting height 5 mm) and one with higher green density (hitting height 55 mm).

2.3 Sintering

Sintering of the water atomized powder was conducted in a small laboratory high temperature furnace (Thermal Technology, 1000-3060-HP20). A burn off/reduction stage at 900 °C was performed in order to remove the lubricant and reduce the oxides. The holding time at sintering temperature was 45 min followed by cooling to 200 °C before removing the samples from the furnace. The heating and cooling rate was 10 °C/min. Three different sintering temperature were evaluated, 1320, 1350 and 1380 °C, respectively. Besides, two different sintering atmospheres, argon and vacuum, were evaluated. Great care was taken in order to ensure as dry sintering atmosphere as possible in order to reduce any decarburisation of the samples. The argon gas was dried in a separate stage before entering the furnace. Before starting heating the vacuum was pumped and the chamber backfilled with argon. The burn off stage was performed in argon for both types of atmospheres after which vacuum was pumped for the vacuum sintering. The vacuum during sintering was kept at 10^{-2} mbar.

2.4 Metallographic characterization

Metallographic characterization of ground and polished cross sections of the reference material and the sintered samples was performed using light optical microscopy (LOM) and scanning electron microscopy/energy dispersive X-ray spectroscopy (SEM/EDS). Care was taken to ensure that all samples were prepared in the same manner using a fully automatic grinding and polishing machine in order to obtain reproducible and relevant data and reduce the influence of preparation induced effects on the analyzed microstructures and porosity level [9]. Soft phases may be deformed easily and thus smeared out covering pores, while hard phases may get fractured in the surface thus showing a porosity higher than the real one. The hardness of the sintered samples was obtained using Rockwell C indentation and Vickers hardness indentation using a load of 10 kg.

3 RESULTS

3.1 Characterization of Stellite 12 reference material

Figure 1 shows the microstructure of the Stellite 12 reference material. As can be seen, two different types of carbides are present in the Co-rich matrix. Based on the contrast obtained in the backscatter electron image (BEI) mode and EDS point analysis of the carbides, see Table 2, it can be concluded that the dark carbide phase corresponds to M_7C_3 (rich in Cr) while the brighter carbide phase corresponds to M_6C (rich in W, but also Cr and Co) [8]. It should be noted that the C-contents given in Table 2 is somewhat uncertain due to the difficulty in quantifying C using EDS. The morphology of the M_6C carbides is equiaxed and angular while the M_7C_3 carbides are more elongated and angular. The size of the major part of the carbides lies in the size interval 10-20 μm . Finally, very few defects such as pores and inclusions were found in the microstructure of the only exception being a very low number of large pores (200-300 μm in diameter). The Rockwell hardness of the Stellite 12 reference material was measured to 44.6 HRC while the Vickers hardness was measured to 510 HV_{10} .

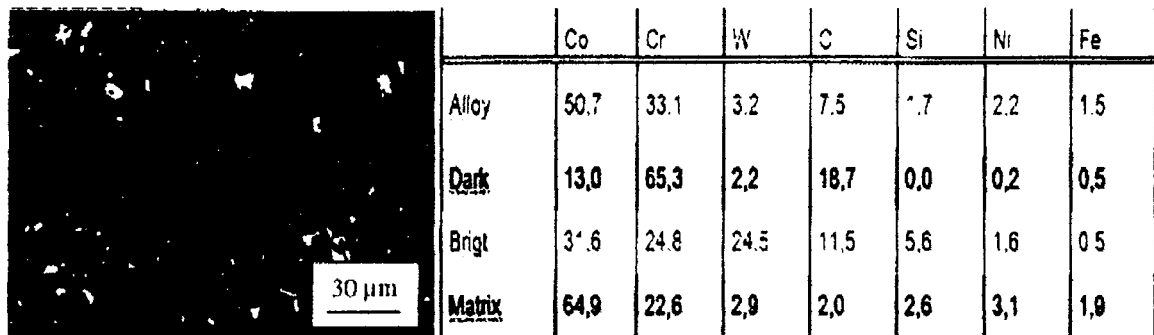


Figure 1. Microstructure (SEM backscatter electron image) and composition (as determined using EDS) of the phases in the Stellite 12 reference material. The microstructure consists of a Co-rich matrix with dark M_7C_3 carbides (rich in Cr) and bright M_6C carbides (rich in W, but also Cr and Co).

3.2 Powder characterization

Figure 2 shows the morphology of the particles of the agglomerated gas atomized and the water atomized Stellite 12 powders. As can be seen, the shape of both the agglomerates of the gas atomized powder particles (spherical in shape) and the water atomized powder is quite irregular as can be expected.

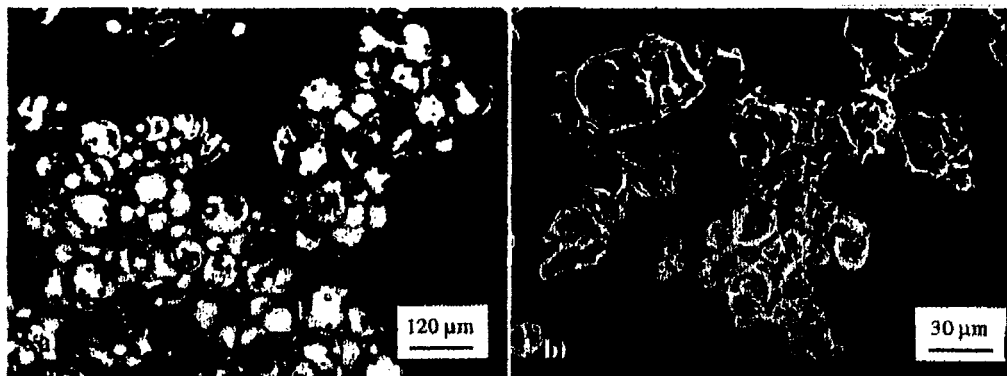


Figure 2. Morphologies of gas atomized powder agglomerates (a) and water atomized powder particles (b).

Comparing the internal structure of the two powders the gas atomized powder particles show no porosity while the water atomized powder particles show a relatively high internal porosity. Furthermore, while the microstructure of the gas atomized powder particles display a significant amount of very small carbides 1-2 μm in size, the water atomized powder, due to the absence of carbon, does not.

3.3 High velocity compaction

High velocity compaction of the agglomerated gas atomized Stellite powder resulted in green bodies of very low quality. Cracking of the green bodies occurred already at low hitting energies and increased in severity when increasing the hitting height. Furthermore, at higher hitting heights ($S > 20$ mm) a phenomenon known as capping started to appear. This is caused by the shockwaves propagation through the green body initiating cracking causing the top part of the compact to separate from the rest of the compact. There are several factors influencing this phenomenon such as the hitting height (compaction energy), the green body elasticity, non homogeneous particle velocities within the green body, etc. [10].

The water atomized Stellite powder resulted in green bodies of very high quality with a high green density and strength. Figure 3 shows the green density of the compacts as a function of hitting height (compaction energy) for samples weighing 50g. As can be seen, density levels close to 95% of the relative theoretical density (RTD) can be obtained using the HVC process. Due to the relatively small samples, the maximum hitting height investigated was limited to 55 mm (corresponding to a hitting height of 2.53 kJ) since higher hitting heights may be harmful to the relatively slim punch used and the fact that the increase in density tend to decrease at higher compaction energies. Besides, material transfer from the Stellite powder to the die surfaces became a problem at higher compaction energies ($S > 30$ mm) causing problems associated with galling. The latter effect is mainly due to two facts. Firstly, cobalt has a high tendency to transfer to the die surfaces something which was observed in a previous study on the high velocity compaction of pure cobalt. Secondly, the die used was slightly worn and consequently had a relatively rough surface which significantly increased the material pick-up tendency. Figure 4 shows fractured cross sections of high velocity compacted green bodies of water atomized powder compacted using a hitting height of 5 and 55 mm, respectively. As can be seen the green body compacted using the higher hitting height displays a more deformed and significantly denser microstructure.

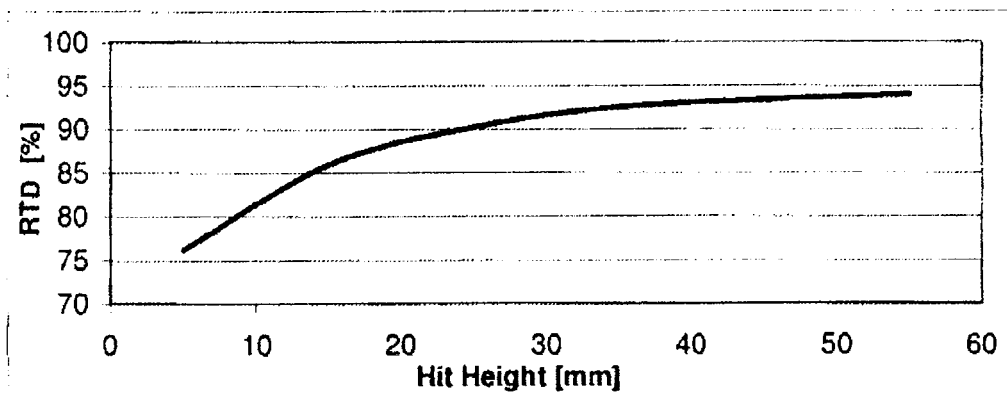


Figure 3. Influence of hitting height on the relative theoretical density (RTD) of high velocity compacted green bodies of water atomized Stellite 12 powder.

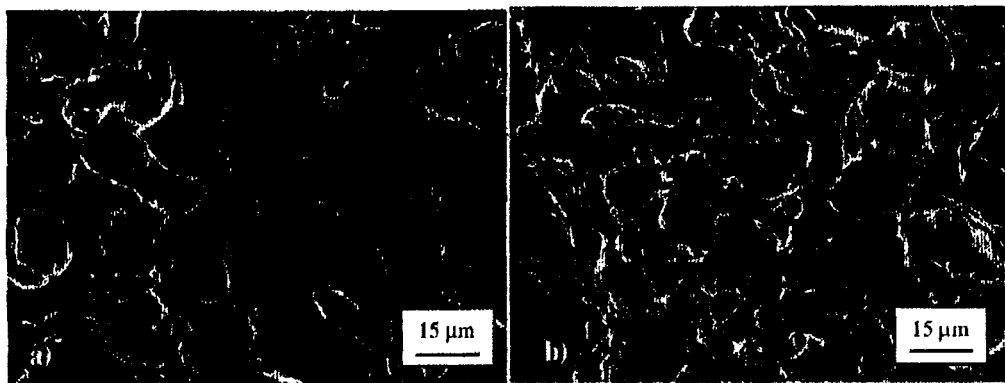


Figure 4. Fracture surfaces showing the microstructure of green bodies water atomized Stellite 12 powder compacted using a hitting height of 5mm (a) and 55 mm (b).

3.4 Characterization of sintered samples

Figures 5 and 6 show polished cross sections of samples sintered in argon and vacuum, respectively. As can be seen, samples sintered in argon show a somewhat higher porosity as compared with samples sintered in vacuum. Furthermore, there is a clear difference in the residual porosity level between the low (hitting height 5 mm) and high green density samples (hitting height 55 mm) although the difference decreases with increasing sintering temperature (increased density). An increased sintering temperature will also affect the resulting microstructure and especially the carbide phase, i.e. carbide size and morphology. At a low sintering temperature, relatively fine, 2-4 μm in diameter, carbides evenly distributed in the microstructure dominate although somewhat larger, 10-20 μm in diameter, carbides can be found. With increasing sintering temperature, the carbides tend to coarsen and concentrate to the grain boundaries and at 1380 $^{\circ}\text{C}$ eutectic M_6C carbides and carbide networks tend to develop at the grain boundaries. This tendency is associated with a coarsening of the grains and a depletion of carbides within the grains, i.e. a more anisotropic microstructure is obtained. This change in microstructure is less pronounced for samples sintered in argon than samples sintered in vacuum and the low green density sample sintered in argon does not display any significant coarsening of the carbide phase and the grain size.

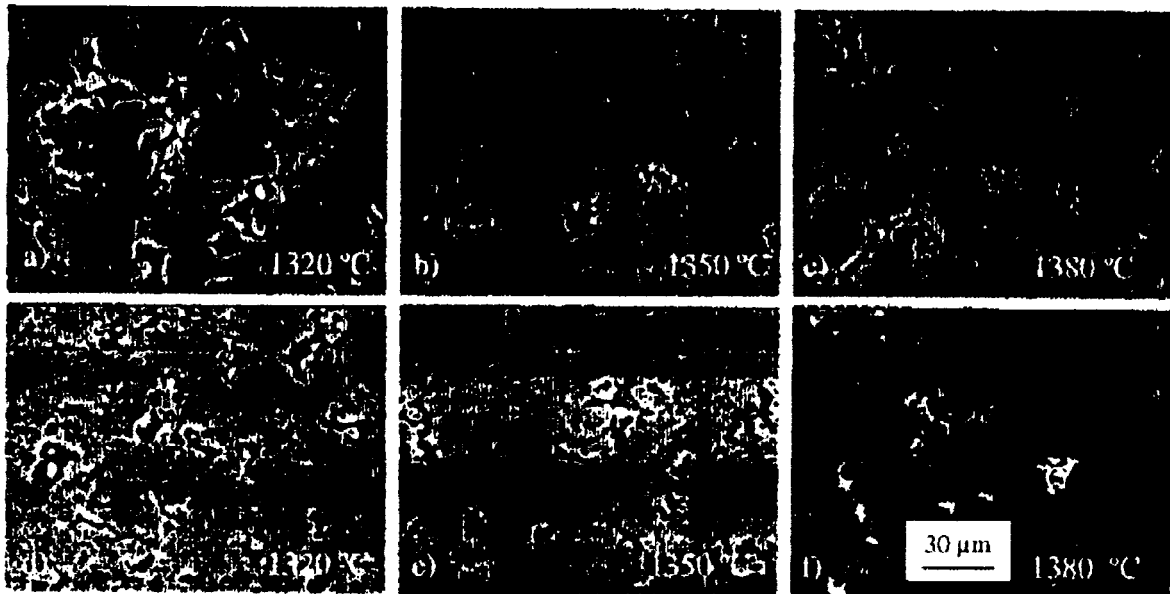


Figure 5. Microstructures of low density samples (a, b and c) and high density samples (d, e and f) sintered in argon as observed in the SEM (backscatter electron image mode).

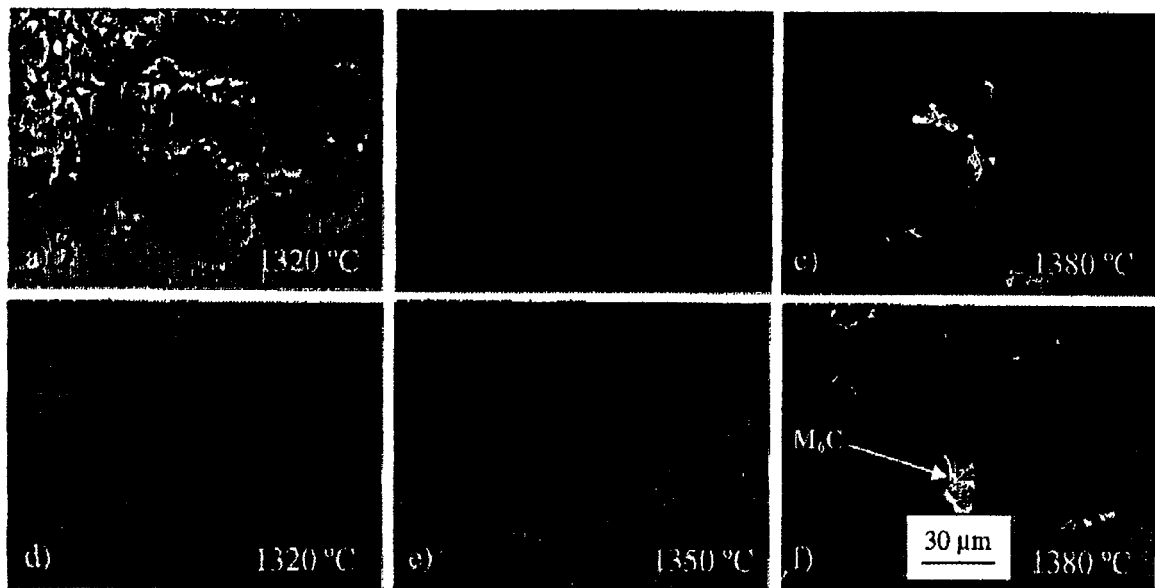


Figure 6. Microstructures of low density (a, b and c) and high density (d, e and f) samples sintered in vacuum as observed in the SEM (backscatter electron image mode).

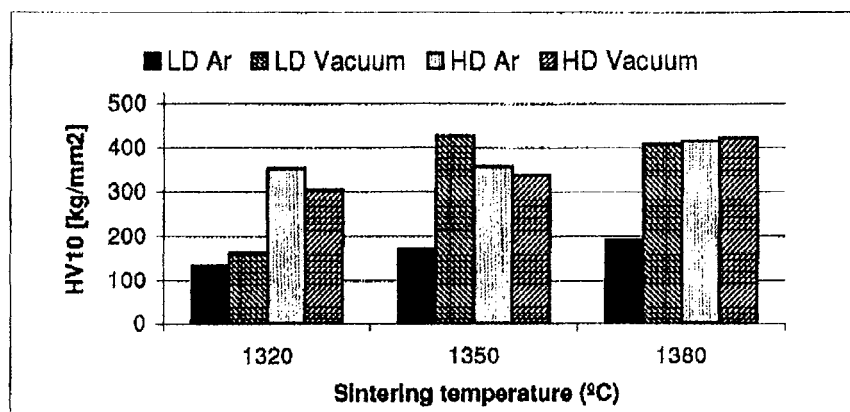


Figure 8. Hardness (HV_{10}) of the sintered Stellite samples at the different sintering temperatures investigated.

4 DISCUSSION

The results obtained in the present study show that high velocity compaction is well suited for the compaction of water atomized Stellite 12 powder to high green densities (95% of the relative theoretical density) although transfer of powder material on the die surfaces was observed at higher compaction energies, resulting in poor surface finish of the green bodies. In contrast, high velocity compaction of the agglomerated gas atomized Stellite 12 powder was associated with problems, mainly due to cracking and capping of the green bodies already at relatively low compaction energies. For this powder, the high amount of binder in combination with the high particle hardness leads to a low green strength due to the absence of cold welding between neighbour particles and the low strength of the binder used. The cracks observed in the green bodies are believed to originate either from the shock waves passing through the green body during the compaction cycle causing an axial loading and unloading cycle of the green body. Besides cracks can also form during the ejection of the component due to spring back, i.e. the radial swelling of the green body when removed from the tool.

As illustrated by the results obtained in the present study, a high green density does not necessarily imply a high as-sintered density. While sintering in argon show a clear correlation between the green density and the resulting as-sintered density this was not the case for sintering in vacuum. The reason for this is not fully understood, but it is believed that a more open pore structure might promote the transportation of gases from the pores which facilitates pore elimination and densification. In contrast, an open pore structure corresponds to a larger surface area which promotes the reduction of oxides. Since the reduction of oxides is associated with the consumption of carbon and carbon has a very strong effect on the melting point of Co, i.e. the addition of 1 wt.% of C to pure Co lowers the melting temperature with 49 °C [8], the an open pore structure may also inhibit the densification process. Also, in order to avoid a coarse microstructure, associated with a large grain size and the formation of eutectic carbides and carbide networks, having a negative impact on the resulting mechanical properties, the amount of liquid phase formed during sintering must be kept to a minimum. In the present study, the samples sintered at 1380 °C, the only exception being the low green density sample sintered in argon, all display a coarse microstructure which indicates that a significant amount of liquid phase has formed during sintering. In these samples, M_6C carbides have precipitated. According to the M_6C rule this type of carbide can precipitate if the W content is high enough (4-6 at.%). In the studied alloy the W content is not high enough to satisfy this rule but still this carbide precipitates. A possible explanation for this is that localized melting can cause the required conditions to be satisfied in areas with a high amount of liquid phase. Furthermore, as found in a previous study on cobalt base alloys [13] the M_6C carbides form on the surface of M_7C_3 carbides. The mechanism of this precipitation is based on the degeneration of the M_7C_3 carbide at elevated temperatures. A possible explanation for the differences in micro structure between the low green density and high green density samples sintered at 1380 °C in argon is a difference in carbon loss during the sintering process. Also, the reason for the low hardness of the sintered samples is most probably attributed to carbon loss during sintering. The lower amount of carbon causes a lower volume fraction of carbides to be precipitated during sintering. In order to compensate for this extra carbon needs to be added to the powder before pressing. However, this will most likely have a strong effect on the sintering temperature due to the fact that carbon will have a strong effect on the liquidus temperature of Co as discussed above.

5 ACKNOWLEDGEMENTS

The authors wish to thank Owe Mårs and Ingrid Hauers at Högåås AB for all the help with supplying the powders and information concerning the sintering process.

6 CONCLUSION

In the present study, the high velocity compaction process has been investigated with respect to its possibility to compact gas atomized and water atomized Stellite 12 powders as well as sintering of high velocity compacted green bodies were investigated. Besides, sintered green bodies of high velocity compacted water atomized Stellite 12 powder have been characterized with respect to as-sintered microstructure and resulting hardness. The main conclusions are:

- High velocity compaction is well suited for the compaction of water atomized Stellite 12 powder resulting in green densities of 95% of the relative theoretical density. In contrast, high velocity compaction of gas atomized Stellite 12 powder is associated with problems, mainly due to cracking and capping of the green bodies already at relatively low compaction energies.
- In order to avoid problems associated with galling during the HVC process, a relatively high amount of an internal lubricant, e.g. a wax, should be added and mixed with the Stellite powder.
- Sintering in vacuum results in a higher as-sintered density as compared with sintering in argon. Under both sintering conditions extra carbon needs to be added to the powder in order to compensate for carbon loss during the sintering process. This is of importance in order to obtain a high hardness of the as-sintered material.
- Of the sintering temperatures investigated, sintering at 1350 °C results in a relatively homogeneous microstructure close to full density with a relatively high hardness. In contrast, sintering at 1320 °C and 1380 °C result in an under sintered (porous) and over sintered (coarse) microstructure, respectively.

7 REFERENCES

1. Malayoglu, U. Mo and W as alloying elements in Co-based alloys - their effects on erosion-corrosion resistance, Wear, vol. 259, no.1, 2005, pp. 219-229
2. Yao, M.X. Wear, corrosion and cracking resistance of some W- or Mo-containing Stellite hardfacing alloys, Materials Science & Engineering A, vol. 407, no.1, 2005, pp. 234-244
3. Waldner, P. Computer-assisted optimization of cobalt-base alloy composition, Journal of Alloys and Compounds, vol. 220, no.1, 1995, pp. 148-151
4. Hamiuddin, Md. Development of wear resistant strong and fully dense Stellite by liquid phase sintering, Powder Metallurgy International, vol. 19, no.1, 1987, pp. 22-26
5. Hauer, I. Properties of high-strength PM materials obtained by different compaction methods in combination with high temperature sintering, Högåås AB, Sweden, 2002
6. Kashanu, H. Effect on temperature on the strain induced phase transformation in Stellite 21 during wear test, Materials Science & Engineering A, vol. 435-436, no.1, 2006, pp. 474-477
7. Guyard, C. Liquid phase sintering as a shaping process for Stellite 6 powder, International Conference on Cobalt: Metallurgy and Uses, vol. II, Brussels; Belgium 10-13 Nov. 1981, pp. 221-228
8. C. T. Sims, Superalloys II, John Wiley & Sons Inc, New York, N.Y., 1987
9. Lawley, A. Metallography of powder metallurgy materials, Materials Characterization, vol. 51, no.1, 2003, pp. 315-327
10. Azhdar, B. Development of a High-Velocity Compaction process for polymer powders, Polymer Testing, vol. 24, no.7, 2005, pp. 909-919
11. Shin, J-C. Effect of molybdenum on the microstructure and wear resistance of cobalt-base Stellite hardfacing alloy, Materials letters, vol. 49, no.1, 2001, pp. 160-164
12. Ashworth, M.A. Microstructure and property relationships in hipped Stellite powders, Powder Metallurgy, vol. 42, no.3, 1999, pp. 243-249
13. Yang, F.M. Secondary M₆C precipitation in K40S cobalt-base alloy, Materials Letters, vol. 49, no.1, 2001, pp. 160-164